JOURNAL OF BACTERIOLOGY, Mar. 2011, p. 1023–1033 Vol. 193, No. 5
0021-9193/11/$12.00 doi:10.1128/JB.01092-10

Identification of an Extracellular Polysaccharide Network Essential for Cytochrome Anchoring and Biofilm Formation in *Geobacter sulfurreducens*▽†

Janet B. Rollefson,[1] Camille S. Stephen,[2] Ming Tien,[2] and Daniel R. Bond[3,4]*

Department of Biochemistry, Molecular Biology, and Biophysics, University of Minnesota, Minneapolis, Minnesota 55455[1]; Center for Environmental Kinetics Analysis, Department of Biochemistry and Molecular Biology, Pennsylvania State University, University Park, Pennsylvania 16802[2]; Department of Microbiology, University of Minnesota, Minneapolis, Minnesota 55455[3]; and BioTechnology Institute, University of Minnesota, St. Paul, Minnesota 55108[4]

Received 13 September 2010/Accepted 9 December 2010

Transposon insertions in *Geobacter sulfurreducens* GSU1501, part of an ATP-dependent exporter within an operon of polysaccharide biosynthesis genes, were previously shown to eliminate insoluble Fe(III) reduction and use of an electrode as an electron acceptor. Replacement of GSU1501 with a kanamycin resistance cassette produced a similarly defective mutant, which could be partially complemented by expression of GSU1500 to GSU1505 in *trans*. The Δ1501 mutant demonstrated limited cell-cell agglutination, enhanced attachment to negatively charged surfaces, and poor attachment to positively charged poly-D-lysine- or Fe(III)-coated surfaces. Wild-type and mutant cells attached to graphite electrodes, but when electrodes were poised at an oxidizing potential inducing a positive surface charge (+0.24 V versus the standard hydrogen electrode [SHE]), Δ1501 mutant cells detached. Scanning electron microscopy revealed fibrils surrounding wild-type *G. sulfurreducens* which were absent from the Δ1501 mutant. Similar amounts of type IV pili and pilus-associated cytochromes were detected on both cell types, but shearing released a stable matrix of *c*-type cytochromes and other proteins bound to polysaccharides. The matrix from the mutant contained 60% less sugar and was nearly devoid of *c*-type cytochromes such as OmcZ. The addition of wild-type extracellular matrix to Δ1501 cultures restored agglutination and Fe(III) reduction. The polysaccharide binding dye Congo red preferentially bound wild-type cells and extracellular matrix material over mutant cells, and Congo red inhibited agglutination and Fe(III) reduction by wild-type cells. These results demonstrate a crucial role for the *xap* (extracellular anchoring polysaccharide) locus in metal oxide attachment, cell-cell agglutination, and localization of essential cytochromes beyond the *Geobacter* outer membrane.

Many dissimilatory Fe(III)-reducing bacteria are able to transfer electrons from cytoplasmic respiratory oxidation reactions to external Fe(III) oxyhydroxides. The predominant Fe(III)-reducing organisms in a variety of anaerobic neutral pH environments belong to the *Geobacteraceae* family of *Deltaproteobacteria* (23, 62, 66). The genetically tractable representative *Geobacter sulfurreducens* (15) can transfer electrons to soluble electron acceptors, such as fumarate and Fe(III) citrate, as well as insoluble electron acceptors, such as Fe(III) and Mn(IV) oxyhydroxides (12). Like most *Geobacteraceae*, it can also use properly poised electrodes as electron acceptors and will form 20- to 40-μm-thick biofilms on such surfaces, with each cell layer able to direct electrons to the electrode via a long-range electron transfer mechanism (8, 46, 47).

To reduce an external electron acceptor such as Fe(III) or an electrode, *Geobacter* must construct a chain of redox proteins linking the outer membrane to the electron-accepting surface (52). Additionally, formation of a network allowing electron transfer between cells is necessary for growth of daughter cells not in contact with Fe(III) particles or to allow new cell layers to grow at a distance from an electrode (46, 47). Genetic studies (10, 37, 40, 50) strongly suggest that *c*-type cytochromes are involved in this process, and electrochemical analysis of electron transfer through electrode-attached biofilms is consistent with a diffusional mechanism involving electron hopping through this biofilm network (21, 46, 47, 60). However, how cytochromes are anchored between cells in a three-dimensional network to create such redox conductivity remains unclear.

G. sulfurreducens type IV pilus and outer membrane *c*-type cytochrome mutants were a focus of early electron transfer and attachment studies, and it was suggested that pili mediated both attachment and long-distance electron conduction (10, 37, 40, 50, 57–59). However, mutants in the structural protein of the type IV pilus (*pilA*) still form thin biofilms and reduce electrodes, showing that other factors contribute to early attachment events and cell surface electron transfer. As *Geobacter* pili are now known to be coated with the hexaheme cytochrome OmcS (38), and the octaheme cytochrome OmcZ is consistently found on material between cells (25, 26), there is increasing evidence that cytochromes localized well beyond the cell membrane play key roles in long-distance electron transfer.

Recently, a library of *G. sulfurreducens* transposon mutants was screened for biofilm and Fe(III) reduction defects (61),

* Corresponding author. Mailing address: BioTechnology Institute, University of Minnesota, 140 Gortner Laboratory, 1479 Gortner Ave., St. Paul, MN 55108. Phone: (612) 624-8619. Fax: (612) 625-1700. E-mail: dbond@umn.edu.

† Supplemental material for this article may be found at http://jb.asm.org/.

▽ Published ahead of print on 17 December 2010.

revealing new genes required for attachment and electron transfer. In particular, a class of biofilm mutants that was unable to reduce insoluble Fe(III) oxyhydroxides and graphite electrodes was identified (61). This class differed from most *c*-type cytochrome and pilus mutants, as mutants did not show any residual electron transfer activity on electrodes and did not show an ability to adapt or evolve to regain metal reduction phenotypes. These mutants contained insertions in open reading frame GSU1501, encoding part of a multisubunit ABC transporter within an operon containing a putative undecaprenyl attachment protein and a series of glycosyltransferase genes, and could not be complemented by expression of just GSU1501 in *trans* (61).

Cuthbertson et al. recently reviewed the role of gene clusters with similar components in synthesis and export of cell surface polysaccharides (16). Variations in outer surface polysaccharides can have pleiotropic effects; sugars can modify surface charge to alter surface attachment, provide an anchor for retention of peripheral proteins, and/or control cell-cell recognition events (5, 20, 29, 30, 39, 65). A complex relationship between extracellular polysaccharides, type IV pili, and biofilm growth is found in *Myxococcus xanthus*, a relative of *Geobacter* with a well-characterized multicellular lifestyle. Fibrils extending from *Myxococcus* cells are comprised of a highly stable protein-polysaccharide matrix, which is required for cell-cell cohesion and social gliding motility (3, 5). Mutants unable to produce this matrix, as well as wild-type cells exposed to Congo red (a carbohydrate binding dye that inhibits fibril polymerization), are blocked in most aspects of cell-cell agglutination and gliding motility (3, 4). Type IV pilus retraction by *M. xanthus* is stimulated by matrix binding, and defects in pili inhibit matrix synthesis via the *dif* signal transduction network (6, 39, 75).

In this work, we describe the phenotype of a newly constructed *G. sulfurreducens* Δ1501 mutant and provide evidence that this mutation disrupts an operon responsible for synthesis of sugars that serve as extracellular anchors for *c*-type cytochromes essential in cell-surface electron transfer. The Δ1501 mutant also displayed an attachment preference for surfaces with a negative charge, further limiting interactions with Fe(III) oxyhydroxides and positively poised electrodes. We report new methods for imaging and isolating a matrix of protein and polysaccharides from *G. sulfurreducens* and show it is both decreased in sugar content and nearly devoid of *c*-type cytochromes in the Δ1501 mutant. This genetic region, containing genes for synthesis of extracellular anchoring polysaccharides (*xapA* to *xapK*), is conserved in all sequenced metal-reducing *Geobacteraceae*. While much work has focused on redox proteins anchored to the membrane, this report shows a role for extracellular polysaccharides as attachment sites for peripheral redox proteins that enable multicellular communities to transfer electrons to distant acceptors.

MATERIALS AND METHODS

Bacterial strains, plasmids, and culture conditions. Bacterial strains and plasmids used in this study are described in Table 1. *G. sulfurreducens* PCA (ATCC 51573) was routinely grown at either 25°C or 30°C in anaerobic mineral medium, with 20 mM acetate as the electron donor and 40 mM fumarate as the electron acceptor (46). To maintain the replacement mutant phenotype, cultures of the Δ1501 mutant were supplemented with kanamycin (200 μg/ml). The Δ1501 mutant containing pGCOMP1500-5 was maintained using gentamicin (20 μg/ml). *Escherichia coli* WM3064, the donor strain used for conjugation (64), was grown in LB broth containing 30 μM 2,6-diaminopimelic acid (DAP) at 37°C, with 10 μg/ml gentamicin present when carrying pBBR1MCS-5 or pGCOMP1500-5.

Construction of the Δ1501 mutant. Single-step gene replacement (40) was used to insert a gene for kanamycin resistance (Kan^r) into *G. sulfurreducens*, replacing GSU1501, with all primers listed in Table 1. Recombinant PCR was used to generate a 2-kb DNA fragment containing Kan^r flanked by approximately 0.5 kb of sequence upstream and downstream of GSU1501. Kan^r was amplified from pBBR1MCS-2 (31) using primers JR07F and JR08R and the following conditions: 30 cycles of 94°C for 1 min, 55°C for 1 min, and 72°C for 2 min, followed by a final extension at 72°C for 10 min. The sequence upstream of GSU1501 was amplified from *G. sulfurreducens* genomic DNA using primers JR03F and JR04R, and the sequence downstream of GSU1501 was amplified using JR05F and JR06R. The following conditions were used for each: 30 cycles of 94°C for 1 min, 52°C for 1 min, 72°C for 1 min, and a final 10-min extension at 72°C. The products of these three PCRs were used as templates in a primerless PCR, producing the 2-kb linear DNA fragment, using 15 cycles of 96°C for 40 s, 47°C for 1 min, 72°C for 5 min, and then a final extension at 72°C for 10 min. The 2-kb fragment was then amplified using 30 cycles of the same reaction conditions and primers JR03F and JR06R. This linear DNA fragment was electroporated into wild-type *G. sulfurreducens* (15), and recombinants were selected on mineral medium containing 200 μg/ml kanamycin. Putative mutants were restreaked on selective medium, and isolated colonies were checked for proper deletions using primers spanning the region. Optical density at 600 nm (OD_{600}) of the wild type and the Δ1501 mutant (using fumarate as the electron acceptor) was monitored for 72 h to verify that there were no growth defects when using fumarate, a soluble electron acceptor.

Construction of a complemented Δ1501 mutant. GSU1500 to GSU1505 were amplified from wild-type *G. sulfurreducens* using primers JR15F and JR16R listed in Table 1 using the following conditions: 30 cycles of 94°C for 1 min, 58°C for 1 min, and 72°C for 6 min, followed by an additional 72°C for 10 min. The ~6-kb fragment was digested and inserted into the XbaI and SacI sites of pBBR1MCS-5, creating the vector pGCOMP1500-5. This construct was mated into the Δ1501 mutant, and transformants were selected on gentamicin (61).

Fe(III) reduction. Wild-type *G. sulfurreducens*, the Δ1501 mutant, and the complemented strain (Δ1501 plus pGCOMP1500-5) were each transferred to mineral medium containing 10 mM acetate as the electron donor and 55 mM Fe(III) citrate or Fe(III) oxyhydroxide as the electron acceptor. Some cultures containing Fe(III) oxyhydroxide as the electron acceptor were supplemented with a 5 μM concentration of the electron shuttle anthraquinone-2,6-disulfonate (AQDS). After inoculation, samples were taken every 2 to 6 h until most Fe(III) had been reduced. A modified colorimetric ferrozine assay was used to measure production of Fe(II) over time (41). Ferrozine reagent (2 g ferrozine/liter in 100 mM HEPES, pH 7) was combined with sample (dissolved in 1 N HCl), and absorbance at 562 nm (A_{562}) was determined. Fe(III) reduction was also monitored in the presence of 50 μg/ml Congo red and 7 μg protein/ml sheared extracellular matrix material where described, with samples taken every 24 h.

Electrochemical analysis. Electrochemical bioreactors were prepared as previously described (46), containing a graphite working electrode, platinum counter electrode, and saturated calomel reference electrode. Reactors were incubated in a 30°C water bath and connected to a 16-channel potentiostat (VMP; Bio-Logic, Knoxville, TN) with EC-Lab software to run chronoamperometry as previously described (46). Anaerobic bioreactors, receiving humidified N_2/CO_2 (80:20 [vol/vol]), were inoculated with 50% (vol/vol) *G. sulfurreducens* entering stationary phase (OD_{600} of 0.4 to 0.5) and mineral medium containing 40 mM acetate (no electron acceptor) and incubated for 24 to 48 h at a potential of +0.24 V or −0.24 V versus the standard hydrogen electrode (SHE). Bioreactors containing two working electrodes were used when the applied potential was varied over the course of the experiment. Bioreactors were first inoculated with 50% (vol/vol) of either wild-type *G. sulfurreducens* or the Δ1501 mutant, approaching stationary phase (OD_{600} of 0.4 to 0.5), in mineral medium containing 40 mM fumarate and 20 mM acetate (potential for acetate oxidation, −0.28 V versus SHE). Cells were allowed to incubate for 24 h at 30°C without an applied potential, after which one of the working electrodes was removed for confocal analysis. Medium was then removed from the bioreactor and replaced with mineral medium containing only 20 mM acetate (no electron acceptor). Electrodes were then poised at either +0.24 V or −0.24 V versus SHE for 4 to 24 h at 30°C, after which the second electrode was removed for confocal analysis. Electrode-attached biofilms were stained using a LIVE/DEAD *Bac*Light bacterial viability kit (Invitrogen Corp., Carlsbad, CA) and imaged using a Nikon C1 spectral imaging confocal microscope (Nikon, Japan).

Biofilm formation assays. To detect attachment phenotypes, cells were grown in mineral medium containing 30 mM acetate for 72 h at 30°C as previously

TABLE 1. Strains, plasmids, and primers used in this study

Strain, plasmid, or primer	Relevant characteristic(s) or sequence (5′ to 3′)	Reference or usage
G. sulfurreducens		
Wild type	ATCC 51573	12
20B5	pMiniHimar RB1 insertion at 1646730, Km^r	61
67B2	pMiniHimar RB1 insertion at 1646910, Km^r	61
Δ1501	Kanamycin resistance gene replacing GSU1501, Km^r	This study
E. coli		
WM3064	Donor strain for conjugation: *thrB1004 pro thi rpsL hsdS lacZ*ΔM15 RP4-1360 Δ(*araBAD*)567 Δ*dapA*1341::[*erm pir*(wt)]	64
Plasmids		
pBBR1MCS-2	Mobilizable broad-host-range plasmid; *lacZ*, Km^r	31
pBBR1MCS-5	Mobilizable broad-host-range plasmid; *lacZ*, Gm^r	31
pGCOMP1500-5	GSU1500 to GSU1505 in MCS of pBBR1MCS-5, Gm^r	This study
Primers		
JR03F	TGATCTGTTGGAATACGGGATGAAGTACCG	PCR amplification of sequence upstream of GSU1501
JR04R	GAAATTCCCCTCTTCAGTTATTCTGAACTC	
JR05F	TTGTGAGCTTCCAAGCATTTCTAAGGATCT	PCR amplification of sequence downstream of GSU1501
JR06R	CACACTGAGGAAGAGCCAGCTCGATATCGG	
JR07F	*TAACTGAAGAGGGGAATTTC*AGCGAACCGGAA TTGCCAGCT	PCR amplification of Kan^r from pBBR1MCS-2, with overhangs homologous to JR04R and JR05F in italics
JR08R	*GAAATGCTTGGAAGCTCACAA*TCAGAAGAACTC GTCAAGAAGGC	
JR09F	GTCCAACAAAGGGAACTGCT	qPCR detection of GSU1501
JR10R	CCTCCGCAGAGAGGTAATCA	
JR11F	AGTTCTCGACGTACGCCACT	qPCR detection of *rpoD*
JR12R	TCAGCTTGTTGATGGTCTCG	
JR13F	CACCGGCATAATCTCCAAGT	qPCR detection of *recA*
JR14R	TTGAGGGATGCGATCTTGCG	
JR15F	TAC*TCTAGA*AATGGTGCCGTTCACCGACCA	PCR amplification of GSU1500 to GSU1505; XbaI and SacI restriction sites in italics
JR16R	GAC*GAGCTC*TCATAAACGAACCTCGTCCC	

described (61). Attachment to the wells of either a Nunclon delta (Nunc 167008)- or a poly-D-lysine-coated (Nunc 152039) polystyrene, flat-bottom, 96-well microtiter plate was determined using a modified crystal violet (CV) assay (53). Cells (or sheared extracellular material) were stained with 0.1% CV for 15 min, plates were rinsed to remove planktonic cells, and the remaining CV was solubilized with dimethyl sulfoxide. OD_{600} was measured as an indicator of attachment level.

Quantitative RT-PCR analysis. Total RNA was isolated from fumarate-grown cells during exponential (OD_{600} of 0.35) and stationary (OD_{600} of 0.60) growth phases and from electrode-grown cells while the current was increasing exponentially and once the current had reached a plateau by using the RNAqueous-Micro kit (Ambion, Austin, TX). The DyNAmo SYBR green two-step quantitative reverse transcription-PCR (qRT-PCR) kit (Finnzymes, Woburn, MA) was used for cDNA synthesis and qPCRs using the manufacturer's protocol and a model 7900HT fast real-time PCR system (Applied Biosystems, Foster City, CA), with *rpoD* and *recA* as internal controls, using the primers listed in Table 1.

Agglutination assay. To test for agglutination phenotypes, cells were grown anaerobically in mineral medium (with excess acetate and limiting fumarate) at 25°C for 72 h, conditions which promote cell aggregation. OD_{600} was first determined for cells which remained in suspension. Then cell aggregates were broken apart by vortexing, and OD_{600} was measured and compared to the initial OD_{600} of the cell suspension to assess the degree of agglutination (59). Additionally, cultures were incubated with Congo red (10 to 50 μg/ml) or extracellular material (7 μg/ml) to test for inhibition and restoration of agglutination, respectively.

Isolation of sheared proteins. To isolate pili, cultures of wild-type *G. sulfurreducens* and the Δ1501 mutant were pelleted and resuspended in 1/100 volume of 1× phosphate-buffered saline (PBS; 137 mM NaCl, 2.7 mM KCl, 4.3 mM Na_2HPO_4, 1.47 mM KH_2PO_4). Suspensions were vortexed vigorously for 2 min to shear loosely bound proteins, and then cells were removed by centrifugation at 16,000 × *g* for 5 min. Supernatants were removed and centrifuged for an additional 25 min, after which the supernatant was collected and 0.1 M $MgCl_2$ was added (from a 1 M stock) to facilitate the precipitation of proteins. After an overnight incubation at 4°C, samples were centrifuged at 30,000 × *g* for 1 h at 4°C (70). To enhance the depolymerization of pili, pellets were resuspended in a small volume of 8 M urea and 50 mM Tris-HCl (pH 8) prior to boiling at 100°C in SDS loading buffer for 15 min, or they would not enter the SDS-PAGE gel. To confirm the identity of isolated pili, bands were excised for in-gel trypsin digestion followed by liquid chromatography-mass spectrometry at the University of Minnesota Center for Mass Spectrometry and Proteomics.

Detection of proteins. Sodium dodecyl sulfate-polyacrylamide gel electrophoresis (SDS-PAGE) (34) in 15% Tris-HCl gels under nonreducing conditions was used to analyze isolated proteins. Samples were boiled at 100°C for 15 min in SDS loading buffer (and treated with urea where indicated), as the longer denaturing times were necessary to visualize pilus proteins and some matrix-bound cytochromes. To detect putative *c*-type cytochromes via peroxidase activity, gels were incubated in 6.3 mM 3,3′,5,5′-tetramethylbenzidine (TMBZ) in methanol (3 parts TMBZ mixed with 7 parts 0.25 M sodium acetate, pH 5.0) for 2 h as previously described (67), after which 30 mM hydrogen peroxide was added. Alternatively, a Pro-Q Emerald 300 glycoprotein gel and blot stain kit (Invitrogen Corp., Carlsbad, CA) was used to visualize glycosylated proteins that had been separated by SDS-PAGE following the manufacturer's procedure. The colloidal blue staining kit (Invitrogen Corp., Carlsbad, CA) was used to visualize total protein.

Fe(III)-coated slides. A solution containing 1% agarose and 0.4 M Fe(III) oxyhydroxide (ferrihydrite) was applied to acid-washed glass slides and allowed to solidify. These Fe(III)-coated slides were then incubated vertically in cultures of wild-type *G. sulfurreducens* or the Δ1501 mutant for 4 h. Attached cells were stained with 100 μg/ml 4′,6-diamidino-2-phenylindole (DAPI) for 5 min and visualized by confocal laser scanning microscopy (CLSM).

Safranin O staining and scanning electron microscopy (SEM) analysis. A graphite electrode was placed in mineral medium (containing 20 mM acetate and 40 mM fumarate) which was then inoculated with wild-type *G. sulfurreducens* or

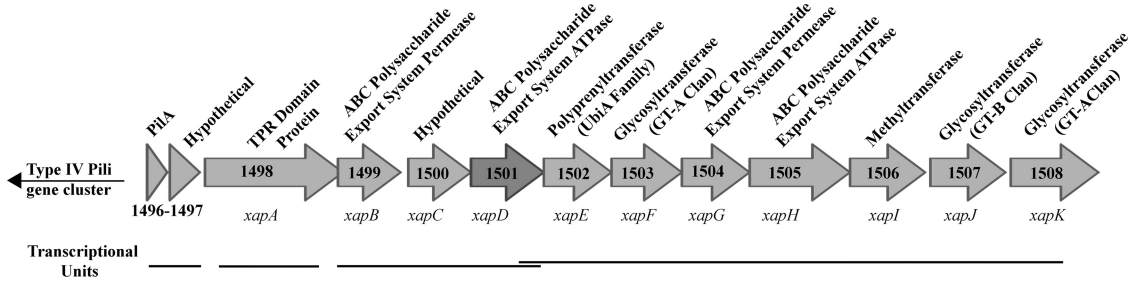

FIG. 1. *G. sulfurreducens* extracellular anchoring polysaccharide (*xap*) cluster (GSU1498 to GSU1508) showing putative gene products and transcriptional units (based on reference 55). GSU1501 and GSU1502 (*xapD* and *xapE*) overlap both transcriptionally and translationally.

the Δ1501 mutant. After 48 h of growth at 30°C, electrode-attached cells were fixed in 2% glutaraldehyde in 0.15 M sodium cacodylate (pH 7.4), for at least 24 h. To help stabilize extracellular polysaccharides, some samples were also fixed in the presence of 0.15% safranin O (19). Samples were then postfixed for 2 h in 1.5% osmium tetroxide and dehydrated in ascending ethanol concentrations (25, 50, 75, 95 [2 times], and 100% [3×], 5 min each) prior to drying by treatment in hexamethyldisilazane (HMDS) (50% [vol/vol] HMDS in 100% ethanol, 100% HMDS [2 times] for 5 min each) (2). Samples were mounted on adhesive carbon films and coated with a thin layer of gold using a Fullam sputter coater (Ernest Fullam Inc., Schenectady, NY) followed by imaging with a Hitachi S3500N variable pressure scanning electron microscope (Hitachi Inc., Toronto, Canada).

Isolation of extracellular matrix. Extracellular material was isolated using a modification of a procedure previously described for *Myxococcus* (13). Briefly, cells were pelleted and resuspended in 1/5 volume of TNE (10 mM Tris-HCl [pH 7.5], 100 mM NaCl, 5 mM EDTA) and blended at low speed for 1 min in a Waring commercial blender (Waring Products, Inc., Torrington, CT). Cells were lysed by the addition of SDS (0.1% final concentration) and stirred at room temperature for 5 min. This lysate had to be further sheared by five passes (~30 s each) through an 18-gauge needle and then centrifuged at 17,000 × *g* for 15 min to obtain a pellet. This pellet was resuspended in Tris-HCl (pH 7.5), pelleted, and resuspended five times to remove SDS. The bicinchoninic acid (BCA) protein assay was used to detect protein (Thermo Scientific, Rockford, IL), and the phenol sulfuric acid method was used to detect carbohydrate with glucose as the standard (48).

Congo red assay. A modification of a previously described Congo red binding assay was used to detect extracellular polysaccharide (35). Suspensions of wild-type *G. sulfurreducens* and the Δ1501 mutant (OD_{600} of 2.0) or extracellular material (100 μg protein/ml) were incubated in the dark with 15 μg/ml Congo red for 30 min at room temperature. Cells were then removed by centrifugation, and absorbance at 490 nm (A_{490}) of the supernatant was measured. Congo red binding was also observed by growing cells on 1.7% (wt/vol) agar plates containing 0.01% (wt/vol) Congo red. Clearing zones around colonies were measured after 5 days of anaerobic growth at 30°C.

Detection of cytochrome reduction. Absorbance of equal concentrations of wild-type, Δ1501 mutant, and Δ1501 plus pGCOMP1500-5 extracellular material was measured using wavelengths spanning 400 to 600 nm. To reduce cytochromes, a few crystals of sodium dithionite were added to each sample, and absorbance was measured.

OmcZ antibody production and purification. Peptides HTSPAAVAKD and DSPNAANLGTVKPGL were selected from the OmcZ protein sequence using an online hydropathicity plot program to identify hydrophilic and antigenic regions (www.vivo.colostate.edu). Subsequently, the peptide sequences were searched against a nonredundant protein database in NCBI protein BLAST to ensure that the peptides matched only OmcZ in *G. sulfurreducens* PCA. A cysteine residue was added to the amino terminus of the first peptide and the carboxyl terminus of the second peptide for conjugation to a carrier protein for antibody production. The peptides were synthesized at Penn State Hershey Macromolecular Core Facility. Polyclonal antibodies to OmcZ were produced in a New Zealand White rabbit (Covance Custom Immunology Services Inc., Princeton, NJ). The peptides were covalently linked to the Sulfolink coupling resin (Pierce Biotechnology, Rockford, IL) via the cysteine residues according to the manufacturer's protocol and used to affinity purify the OmcZ antibodies from the antiserum. The following modifications for affinity purification of the antibodies were obtained from the Pikaard Lab (Washington University): the resin was washed with 20 ml 1× PBS with 250 mM NaCl, pH 7.2, and then with 10 ml of 100 mM glycine, pH 2.5 elution buffer, and finally 20 ml 1× PBS, pH 7.2. The antiserum was diluted with an equal volume of 1× PBS, pH 7.2, and allowed to incubate overnight with the Sulfolink resin at 4°C with gentle rotation. After binding of the antibodies, the resin was washed with 20 ml 1× PBS, pH 7.2, and 10 ml 1× PBS, pH 7.2, with 250 mM NaCl. The antibodies were eluted with 5 ml of elution buffer, in 500-μl aliquots, and neutralized with 50 μl of 1 M Tris, pH 8. Aliquots containing the antibody were detected using the Bradford reagent (9). OmcZ specificity was tested via Western blotting of *G. sulfurreducens* biofilm-grown cells, showing only one cross-reactive band.

Detection of OmcZ in extracellular material. Protein content of wild-type and Δ1501 extracellular material was determined using the Lowry protein assay (43). For SDS-PAGE, 28 μg of protein was suspended in sample buffer and boiled for 15 min prior to electrophoresis on a 12% gel (34). The proteins were then transferred onto a nitrocellulose membrane and probed with a 1:100 dilution of affinity-purified OmcZ antibody. The blot was then developed using a BCIP/NBT solution (Amresco, Solon, OH).

RESULTS

Identification of the extracellular anchoring polysaccharide (*xap*) gene cluster and construction of a GSU1501 replacement mutant. Previous screening of a transposon library for increased surface adherence in a 96-well crystal violet assay identified two mutants with transposon insertions in open reading frame GSU1501 (Fig. 1) that demonstrated a growth impairment with Fe(III) oxyhydroxides and graphite electrodes as electron acceptors (61). The original GSU1501 transposon mutants could not be complemented through reintroduction of GSU1501 (61), consistent with the location of this gene within a larger transcriptional unit (32, 55). For further work with this locus, a new mutant was constructed via complete deletion of GSU1501 and replacement with a kanamycin resistance cassette. Fe(III) oxyhydroxide reduction and attachment to electron-accepting electrodes could not be restored in the Δ1501 mutant via expression of GSU1501 alone or by expression of GSU1500 to GSU1502. However, expression of multiple genes from this cluster (GSU1500 to GSU1505) in the Δ1501 mutant restored most phenotypes, such as Fe(III) oxyhydroxide reduction and surface attachment, to within 50% of that of the wild type (detailed in Fig. S1 in the supplemental material).

Altered cell-cell agglutination and lack of binding to positively charged surfaces. During routine cultivation, it was observed that, unlike wild-type *G. sulfurreducens*, the Δ1501 mutant failed to aggregate and accumulate at the bottom of culture tubes upon reaching stationary phase with fumarate as the electron acceptor. This difference was more pronounced at 25°C, a temperature previously reported to facilitate agglutination of *G. sulfurreducens* (57, 59). At 25°C, compared to the Δ1501 mutant, 5-fold more wild-type cells agglutinated (Fig.

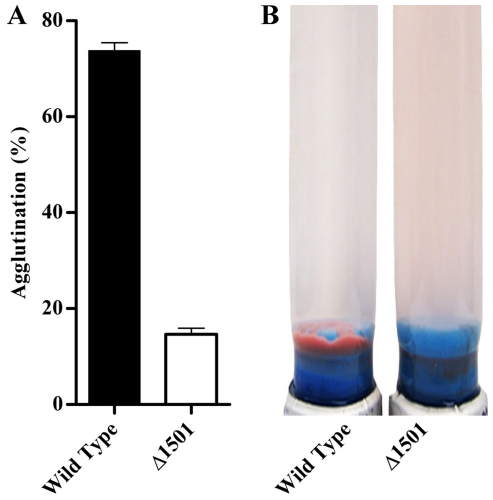

FIG. 2. (A) Percent agglutination in wild-type *G. sulfurreducens* and the Δ1501 mutant as determined by a change in OD_{600} before and after aggregate disruption. Error bars represent standard errors of the means of results for three replicates. (B) Agglutinated cells after 72 h of growth at 25°C.

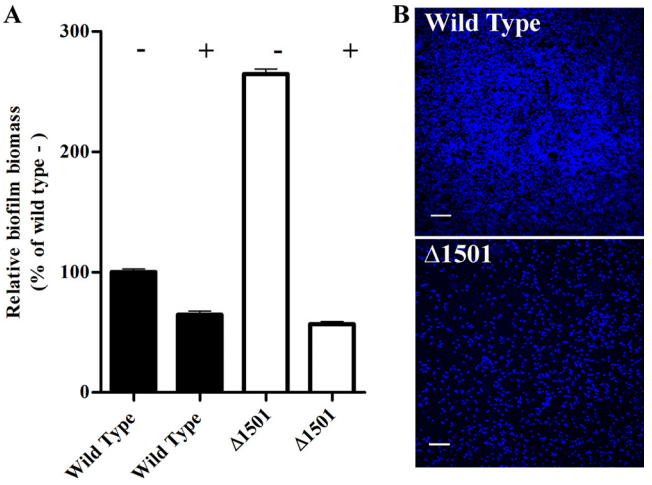

FIG. 3. (A) Biofilm formation based on crystal violet staining of cells adherent to negatively (−) or positively (+) charged 96-well plates, with mean absorbance expressed relative to wild-type attachment to negatively charged plates. Error bars represent standard errors of the means of results for three replicates. (B) Representative CLSM images of wild-type *G. sulfurreducens* and Δ1501 mutant attachment to Fe(III) oxyhydroxide-coated glass slides after 4 h of attachment. Panels are maximum projections (bar, 20 μm) of attached cells stained with DAPI.

2). The ability to agglutinate was partially restored through expression of GSU1500 to GSU1505 (Fig. S1A). This defect in cell-cell attachment was surprising, as the mutant was first identified based on an increased biofilm formation phenotype.

Adherence to 96-well plates was reexamined, comparing negatively charged and positively charged poly-D-lysine-coated wells. The mutant demonstrated nearly 3-fold-higher attachment to negatively charged plates, compared to positively charged poly-D-lysine-coated plates (Fig. 3A). Attachment, measured using crystal violet, reflected actual biomass on the surfaces, as similar results were obtained with a protein assay (data not shown). This suggested that the mutant was highly attracted to negatively charged surfaces in comparison to the wild type, which explained its identification in the transposon screen.

Fe(III) oxyhydroxides are known for their positive surface charge, a property that makes them excellent materials for sorption of AsO_4^{3-} and PO_4^{3-} ions (1, 56). When attachment to vertically positioned Fe(III)-coated slides was investigated, very few Δ1501 mutant cells attached to Fe(III)-coated slides in comparison to the number of wild-type cells (Fig. 3B). Consistent with this observation, when the mutant was cultivated with Fe(III) oxyhydroxide as an electron acceptor, less than 5 mM Fe(III) was reduced after 7 days, compared to 50 mM in the wild type (Fig. 4). In the presence of only 5 μM AQDS, an electron-shuttling compound able to transfer electrons from multiple membrane- and surface-associated redox proteins to Fe(III) oxyhydroxides (71), the mutant was capable of wild-type rates of Fe(III) reduction (Fig. 4). Along with the observation that the mutant exhibited wild-type rates of soluble Fe(III) citrate reduction (61), this suggested that the phenotype was not due to a defect in electron transfer proteins bringing electrons to the outer membrane but rather was related to cell-surface attachment or electron transfer events beyond the cell membrane.

Electrode binding deficiency is also linked to surface charge. Previous work showed that GSU1501 transposon mutants failed to produce an electrical current when provided with electrodes as electron acceptors (61). Since this mutation did not affect the mutant's ability to transfer electrons to soluble metals and AQDS, we hypothesized that the electrode phenotype was also linked to attachment. When bare electrodes were used in an attachment assay but not poised to act as electron acceptors, both wild-type *G. sulfurreducens* and the Δ1501 mutant attached (Fig. 5A and D). As cells remained attached after rinsing in fresh medium, incubation in another change of buffer for staining, and mounting for imaging, the results of these experiments initially appeared to contradict the hypothesis that the mutant was unable to attach to electrodes.

However, when these same electrodes were poised to act as

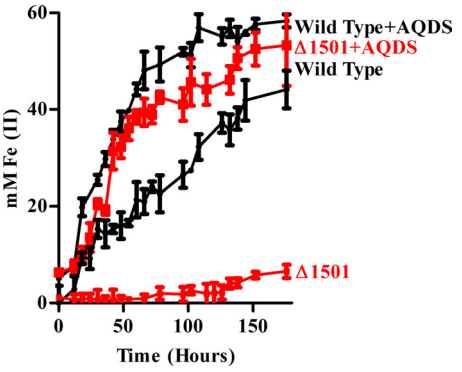

FIG. 4. Iron reduction curves showing Fe(III) oxyhydroxide reduction over time as indicated by accumulation of Fe(II) in the presence and absence of soluble electron shuttle AQDS (5 μM). Error bars represent standard errors of the means of results for three independent replicates.

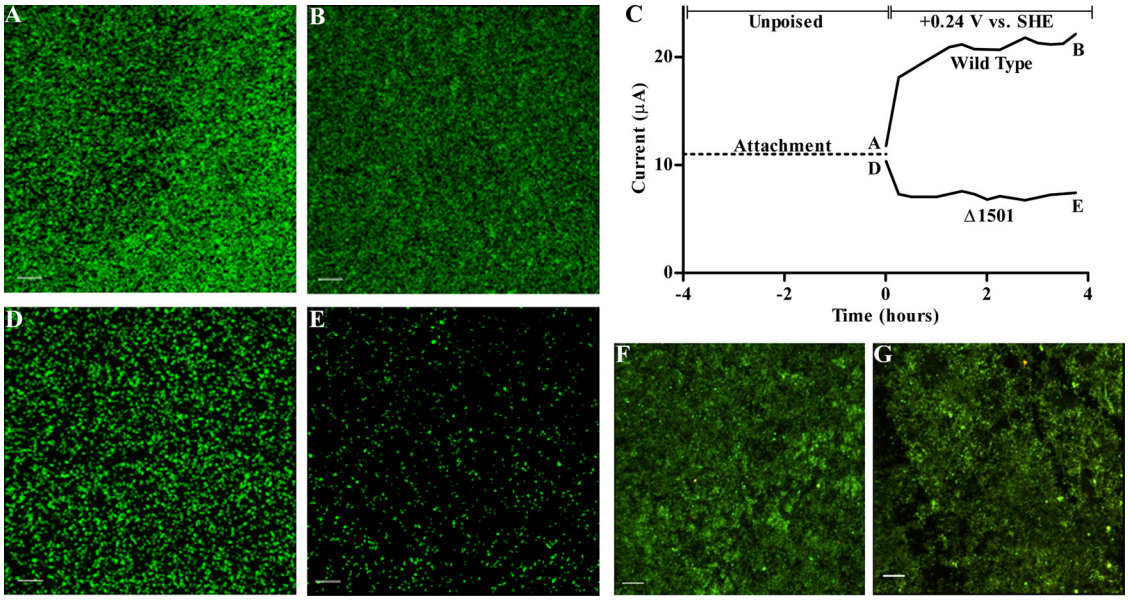

FIG. 5. CLSM images of biofilm formation by wild-type *G. sulfurreducens* (A) and the Δ1501 mutant (D) after 24 h of attachment to unpoised graphite electrodes, followed by images taken of the wild type (B) and the Δ1501 mutant (E) after four additional hours with electrodes poised at +0.24 V versus SHE. (C) Current production during 4 h poised at +0.24 V versus SHE; letters indicate CLSM time points. CLSM images of the wild type (F) and Δ1501 mutant (G) after 24 h with electrode poised at −0.24 V versus SHE. CLSM images are maximum projections (bar, 20 μm) of electrode-attached biofilms stained with a LIVE/DEAD kit.

oxidizing electron acceptors (at +0.24 V versus SHE), a condition which withdraws electrons and alters the surface charge to become more positive, Δ1501 mutant cells rapidly detached. Figure 5 shows an example experiment, where unpoised electrodes were precolonized for 24 h, planktonic cells were washed from the reactor, and a subset was imaged (Fig. 5A and D). Electrode surfaces were then poised at +0.24 V versus SHE for only 4 h before imaging (Fig. 5B and E). During this time, wild-type cells remained attached to electrodes, while the number of attached mutant cells severely decreased (Fig. 5B versus E).

When precolonized electrode surfaces were poised at a negative potential (−0.24 V versus SHE), for as long as 24 h, both the wild type and the Δ1501 mutant remained attached (Fig. 5F and G). The ability to attach to a positively charged electrode was restored when GSU1500 to GSU1505 were reintroduced to the Δ1501 mutant (Fig. S1B). These experiments further demonstrated that attachment of the Δ1501 mutant was a function of electrode surface potential.

GSU1501 expression is similar during planktonic exponential growth with fumarate and biofilm growth with electrodes. GSU1501 mRNA expression levels were measured via quantitative RT-PCR to determine if this gene was specifically induced during growth with different electron acceptors, using both *rpoD* and *recA* as standards. GSU1501 expression was not significantly higher when cells were grown as biofilms (in exponential phase) on oxidizing electrodes than when exponentially grown as fumarate-reducing cultures. Regardless of the electron acceptor, expression levels dropped as cells entered into stationary phase (decreasing 80-fold as planktonic cells abruptly entered stationary phase due to fumarate depletion). These wild-type *G. sulfurreducens* mRNA expression levels showed that solid-phase electron acceptors were not needed to induce GSU1501 expression and were consistent with the fact that cells pregrown with fumarate demonstrated the strong phenotypes of poor attachment and cell-cell agglutination.

SEM evidence that Δ1501 mutants lack an extracellular fibrillar matrix. GSU1501 is a component of a putative ATP-dependent exporter within an operon annotated to have a series of glycosyltransferases similar to those used to assemble extracellular polysaccharides (Fig. 1). As *Geobacter* lacks O-antigen side chains (69), we hypothesized that this cluster was involved in synthesis and export of sugars to the cell exterior, leading to a change on the mutant cell surface, or on exposed proteins, that prevented electron transfer to metals or electrodes.

Recent work with pathogens such as *Enterococcus faecalis* has shown that common fixation methods for scanning electron microscopy fail to preserve delicate outer surface structures but that treatment with some dyes can enhance stabilization and visualization of extracellular fibrils (19). After screening a range of commonly used agents, we found that if *Geobacter* cells were fixed in the presence of the small-molecular-weight dye safranin O, which is typically used to stain negatively charged mucopolysaccharides (63), significantly more detail was preserved.

The first set of SEM images shown in Fig. 6 compares mutant and wild-type cells attached to unpoised graphite surfaces, using standard SEM preparation protocols (Fig. 6A and B). The second series of images shows biofilms prepared using safranin O in the fixative (Fig. 6C and D). In both cases, individual cells attached to the electrode surface were visible, but safranin preserved a dense network of extracellular material surrounding wild-type cells (Fig. 6C). This fibrillar network was absent from the Δ1501 mutant under all conditions tested (Fig. 6B and D).

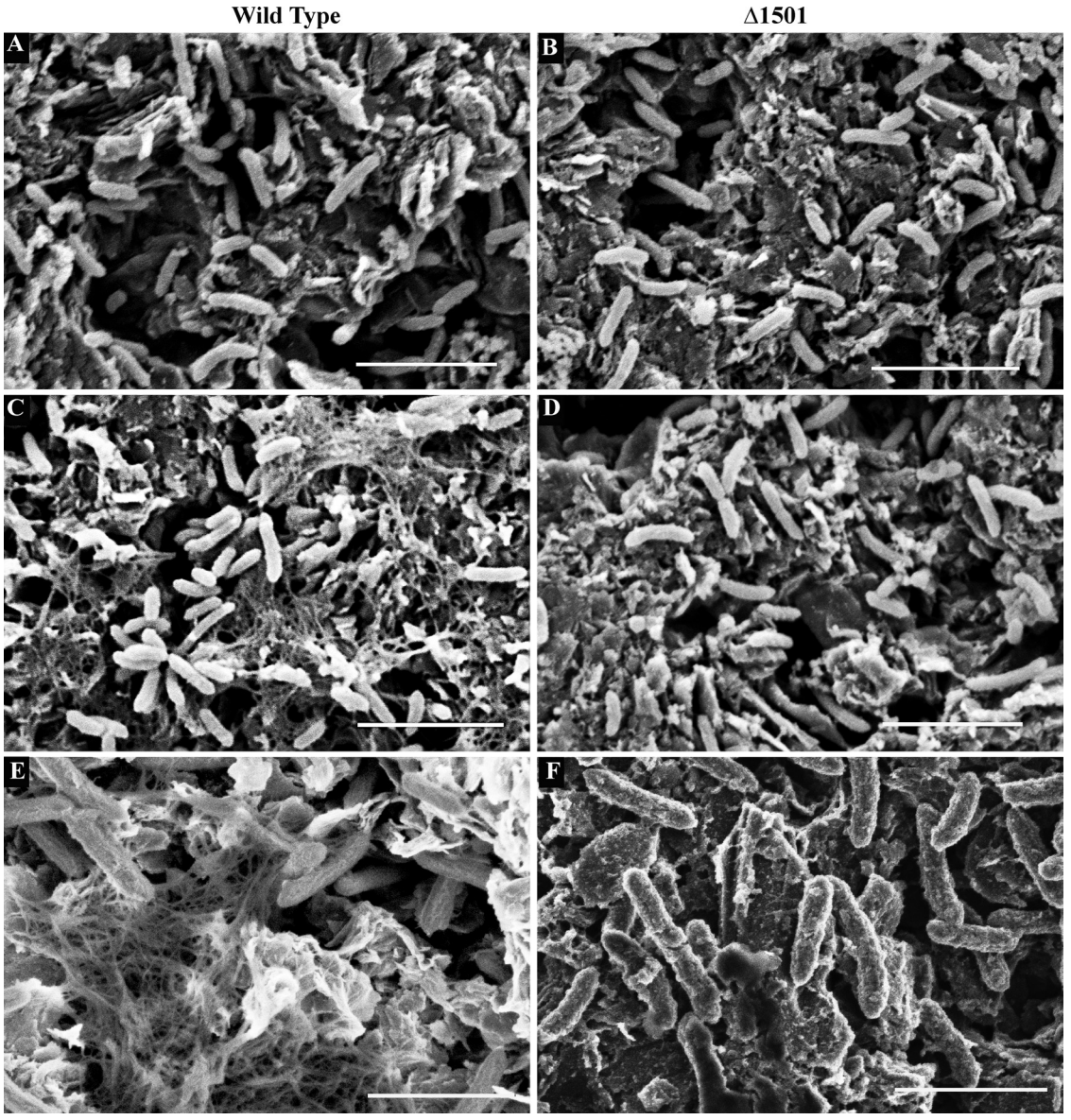

FIG. 6. SEM images of wild-type *G. sulfurreducens* (A) and Δ1501 mutant (B) biofilms and wild-type (C) and Δ1501 mutant (D) biofilms fixed in the presence of cationic dye safranin O (bar, 5 μm). Field emission SEM images of wild-type (E) and Δ1501 mutant (F) biofilms (bar, 2 μm). All biofilms were grown on unpoised graphite electrodes.

When biofilms were imaged using a more sensitive 2.5-kV field emission scanning electron microscope, fibrils surrounding wild-type cells could also be seen in preparations lacking stabilizing dyes (Fig. 6E). Even with this more sensitive microscope, no material or fibrils were detected around the mutant (Fig. 6F). In all cases, the diameters of these fibrils were larger than what has been reported for *Geobacter* pili (20 to 40 nm) (57).

As mutations in type IV pili are known to affect agglutination, Fe(III) reduction, and electrode growth (57–59) and pili could aggregate to form larger fibrils during preparation for SEM, cells were sheared to obtain pili. Sheared fractions from both mutant and wild-type cultures had to be resolubilized in 8 M urea to visualize individual proteins by SDS-PAGE. Urea-solubilized pellets from wild-type and mutant cultures produced similar bands corresponding to the predicted 6-kDa size of processed PilA subunits. Mass spectrometry revealed that processed PilA protein represented the dominant sequence recovered from this 6-kDa band in all cases (data not shown).

Staining to label putatively glycosylated proteins, using safranin O or periodic acid oxidation, and labeling with fluorescent detection reagents consistently stained this PilA subunit band as well as an unidentified 15-kDa protein in both preparations (data not shown). In addition, all pilus preparations contained a large amount of a 50-kDa protein that stained positive for heme, consistent with the recent discovery that the 50-kDa OmcS cytochrome coats *Geobacter* type IV pili (38). As we could detect no difference in the abundances of pili, their glycosylation states, or the abundances of pilus-associated proteins, these results indicated that the fibril material

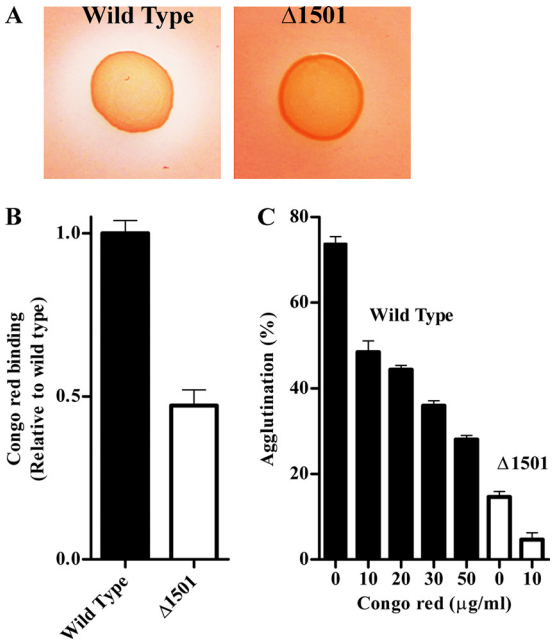

FIG. 7. (A) Colonies of wild-type *G. sulfurreducens* and the Δ1501 mutant grown on agar plates supplemented with Congo red. (B) Congo red binding as an indicator of relative levels of extracellular material. (C) Inhibition of wild-type agglutination with increasing concentrations of Congo red, compared to agglutination in the Δ1501 mutant. Error bars represent standard errors of the means of results for three replicates.

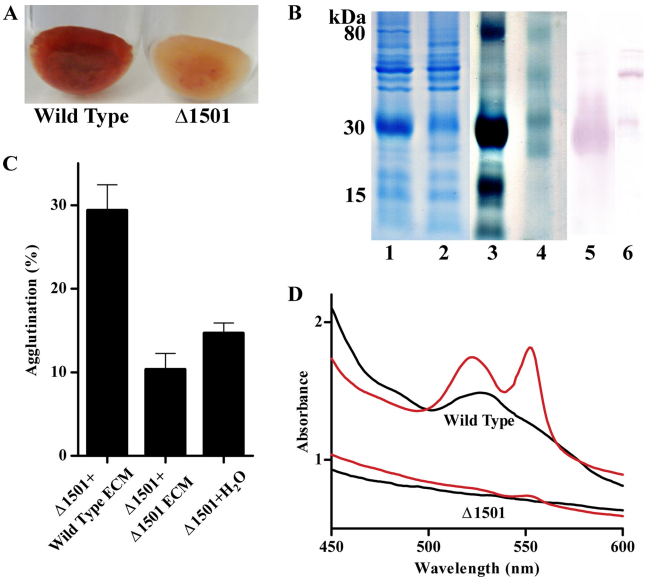

FIG. 8. (A) Extracellular material isolated from the wild type and Δ1501 mutant. (B) Total extracellular protein in matrix from the wild type (lane 1) and Δ1501 mutant (lane 2) and a heme stain of the wild type (lane 3) and Δ1501 (lane 4, containing twice as much material as lane 3) and an anti-OmcZ Western blot of the wild type (lane 5) and Δ1501 mutant (lane 6), with 20 μg protein loaded in lanes 1 to 3, 40 μg in lane 4, and 28 μg in lanes 5 and 6. (C) Percent agglutination of the Δ1501 mutant with the addition of extracellular material (7 μg/ml) isolated from either the wild type or the mutant. Error bars represent standard errors of the means of results for four replicates. (D) UV/visible spectra of isolated extracellular material. Oxidized, black; dithionite reduced, red.

missing in the Δ1501 mutant was not related to type IV pili. Abundant fibrils extending from cells have also been observed in *Geobacter* mutants lacking the pilin protein PilA (28), further supporting this conclusion.

Congo red binding evidence for an extracellular polysaccharide matrix defect in Δ1501. In the related deltaproteobacterium *M. xanthus*, polysaccharide fibrils polymerize to form a matrix anchoring proteins to the outer surface, and this matrix also acts as a signal for cell-cell recognition and pilus retraction (5, 39, 65). Polysaccharide binding dyes, such as Congo red, adhere to this matrix and have the notable effect of preventing fibril polymerization and cell-cell agglutination (3, 4). Based on the hypothesis that the Δ1501 mutant was defective in production of a similar kind of matrix, the effect of dye binding to cells was investigated.

On agar plates supplemented with Congo red, wild-type *G. sulfurreducens* colonies developed clearing zones, extending as much as 0.37 (±0.041 [standard deviation]) cm from colony edges, while little clearing was observed around colonies of the Δ1501 mutant (Fig. 7A). As clearing zones could indicate either reductive fission to aromatic amines or binding of Congo red, a nonrespiratory binding assay was performed (35). After growth to stationary phase in liquid culture, wild-type *G. sulfurreducens* bound twice as much Congo red as the Δ1501 mutant (Fig. 7B), even after pelleting and resuspension in aerobic buffer, showing that this Congo red binding material was cell associated and did not require respiration for the phenotype.

Growth of wild-type *G. sulfurreducens* in medium containing Congo red did not affect growth rate or final cell density, but supplementation of 50 μg/ml Congo red inhibited cell-cell agglutination by the wild type nearly to the level seen in the Δ1501 mutant without Congo red (Fig. 7C). As little as 10 μg/ml Congo red eliminated the agglutination that remained in the Δ1501 mutant. In addition, Fe(III) oxyhydroxide reduction by wild-type cultures was decreased in the presence of Congo red, with only 20 mM Fe(II) produced after 7 days, compared to 50 mM when Congo red was not present.

Isolation of the extracellular matrix from wild-type and Δ1501 mutant cultures. Using a protocol based on methods used to extract *Myxococcus* fibrils, involving mechanical shearing, SDS treatment, and pelleting of high-molecular-weight material, a thick red pellet was obtained from wild-type *G. sulfurreducens* cells. Analysis of three independent preparations showed that this material contained both protein and polysaccharide in a nearly 1:1 ratio in the wild type, and an average of 7.5 mg (on a protein basis) was obtained from 1 liter of *G. sulfurreducens* stationary-phase fumarate-grown culture (~150 mg protein). In contrast, the mutant produced less total material, the isolated matrix contained approximately 60% less polysaccharide per unit of protein (0.57:1), and it was largely absent of color (Fig. 8A). Expression of GSU1500 to GSU1505 in the Δ1501 mutant resulted in an increased matrix polysaccharide content per unit of protein (0.77:1) and restoration of the color of wild-type matrix material (Fig. S1C).

Consistent with whole-cell Congo red binding assays, Δ1501 extracellular material bound less Congo red than the wild type (20%, per unit of protein). Compared to the matrix from the

wild type, the extracellular matrix from the Δ1501 mutant also showed a preference for binding negatively charged surfaces. Using bound protein as a measure of attachment, nearly 2-fold more matrix material from the Δ1501 mutant attached to negatively charged surfaces than wild-type material (data not shown). Taken together, these data revealed the presence a high-molecular-weight extracellular matrix, which retained a protein component even in the presence of SDS, that was significantly altered in the Δ1501 mutant in sugar content, charge, and Congo red binding.

Both in-gel peroxidase staining and UV/visible spectral analysis revealed that extracellular material from the Δ1501 mutant was nearly devoid of *c*-type cytochromes compared to that from the wild type (Fig. 8B and D). In fact, to detect residual cytochromes in mutant preparations, twice as much material had to be loaded onto PAGE gels (e.g., Fig. 8B, lane 4). In studying this isolated matrix, we also noted that, in order to release proteins for separation and visualization, much longer (15-min) boiling times at 100°C in SDS loading buffer were required; otherwise, the majority of the material remained in the well or near the top of the gel. When properly separated, the most abundant heme-positive protein in the wild-type matrix had an estimated size of 25 to 30 kDa, a size range suggesting the processed form of the *c*-type cytochrome OmcZ (25, 26, 51) as well as the *c*-type cytochrome OmcE (50).

Western blot analysis of isolated matrix material from wild-type cells confirmed the presence of the processed OmcZ and found significantly less OmcZ in the Δ1501 matrix (Fig. 8B). Additionally, when using a high concentration of antiserum, a faint band for the 50-kDa form of OmcZ could be seen, but only in the Δ1501 matrix. These results confirmed that OmcZ was a major constituent missing from the Δ1501 matrix, and what little OmcZ protein remained was processed differently. Unidentified cytochromes in the ~90-kDa, 15-kDa, and 8-kDa ranges were also missing, suggesting that multiple cytochromes were typically anchored in this network.

The wild-type extracellular matrix added to the Δ1501 mutant partially restores key phenotypes. Extracellular material, sheared from cells in the presence of SDS and then washed to remove detergent (Fig. 8A), was added back to cultures at physiological concentrations (7.5 mg/liter). Even though this material had been sheared and washed in detergent, the addition of the wild-type matrix restored the mutant to ~40% of wild-type agglutination levels (Fig. 8). In contrast, the addition of the same material isolated from the Δ1501 mutant did not increase agglutination of either the wild type or the mutant, even at twice these added levels (data not shown). Similarly, the addition of the wild-type matrix material to Fe(III) oxyhydroxide medium partially restored the ability of the mutant to reduce Fe(III), with 30 mM Fe(II) produced after 1 week compared to only 5 mM produced by cultures of the Δ1501 mutant, even in the presence of the additional matrix from the mutant (data not shown).

DISCUSSION

This work demonstrated that an extracellular matrix, rich in cytochromes and polysaccharides, is produced by *G. sulfurreducens*. Deletion of a gene (Δ1501) within a cluster of putative polysaccharide biosynthesis proteins (Fig. 1) led to defects in the sugar content, charge, and dye binding properties of this matrix, as well as the cytochrome content. Because this gene cluster (GSU1498 to GSU1508) was implicated in the production of extracellular anchoring polysaccharides, we proposed the designation *xap* for this locus. Along with the ATP-dependent exporter disrupted by the *xapD* mutation, this region also contains a complement of GT-A family (NDP-utilizing) glycosyltransferases, a UbiA-like prenyltransferase likely used to anchor polysaccharide chains to undecaprenyl carriers in the cytoplasmic membrane, and a periplasmic TPR domain-containing protein weakly similar to proteins found in glycosylation pathways (33) and polysaccharide export pathways (27).

Many *Geobacter c*-type cytochrome mutants and pilus mutants remain able to attach to surfaces, transfer electrons to electrodes, or adapt over time to achieve wild-type reduction rates (22, 36, 50, 51, 58). In contrast, the Δ1501 (*xapD*) mutant failed to form even thin biofilms on electron-accepting electrodes, never demonstrated more than 1% of wild-type electron transfer rates (5 $\mu A/cm^2$) at an electrode, and retained this phenotype regardless of extended exposure to Fe(III) or electrodes. Mutant cells still produced pili, as well as cytochromes attached to the pili, and retained the ability to transfer electrons to external, soluble acceptors. This stable phenotype suggested that the *xap* locus represented a central yet previously unstudied aspect of *G. sulfurreducens* electron transfer that was unrelated to transmembrane electron transfer or pili.

It was previously noted that attachment in the 96-well-plate-based biofilm assay was not a good predictor of the ability to form electrode-attached biofilms (61). This can now be explained by the positive surface charge of the electrode when poised, in contrast to the negatively charged polystyrene plates used to discover increased adherence in most screening assays. Surface charge of a bacterial cell and electrostatic interactions are factors known to be important in biofilm formation, with the charge of the surface itself critical in the initial attachment stage (14, 17, 44, 49, 54). The surface of wild-type *G. sulfurreducens* has been reported to be electronegative, with a zeta potential similar to most *Shewanella* species (29), which likely evolved for contact with positively charged metal oxyhydroxides and may explain why many *Geobacter* strains easily attach to commonly used anode surfaces.

Polysaccharides located outside the bacterial membrane are common agents used to mediate surface attachment and cell-to-cell biofilm interactions (18, 20, 24, 72, 73), as they are cheap to polymerize (compared to the ATP cost of peptide bond synthesis) and easy to modify. The fibrils occasionally visualized extending from *Geobacter* cells have been the subject of speculation, most commonly that they represent pilus- or pseudopilus-based structures (28). However, we found that this fibril network surrounding wild-type *G. sulfurreducens* bound polysaccharide binding cationic dyes and that disruption of the *xap* polysaccharide biosynthesis locus (which did not appear to affect pili) eliminated these fibrils.

It would seem counterintuitive for *Geobacter*, which depends upon extracellular electron transfer events between membrane proteins and surfaces, to coat itself in a layer of potentially insulating sugars. Our demonstration that this matrix is rich in *c*-type cytochromes, in particular OmcZ (25, 26, 51), suggests that this matrix is not insulating and is instead a scaffold for electron transport proteins. Such a framework for tethering

cytochromes is consistent with multiple electrochemical studies demonstrating that electrons hop through the *Geobacter* biofilm network according to semiinfinite diffusional kinetics (21, 46, 47, 60). Along with the recent demonstration that *G. sulfurreducens* type IV pili are coated in cytochromes (38), this provides further evidence that electron transfer from *G. sulfurreducens* to surfaces requires cytochromes localized well beyond the cell membrane. The anchoring of cytochromes in extracellular matrix may be a general characteristic of metal-reducing microorganisms, as *S. oneidensis* MR-1 cytochromes have also been detected beyond the cell and in the extracellular matrix (42, 45).

While the *xap* mutation did not appear to alter pilus assembly, the *xap* cluster is located immediately downstream of the type IV pilus operon in all sequenced *Geobacter* strains, suggesting a secondary interaction or coordination between pili and this component of the *Geobacter* extracellular matrix. In particular, GSU1500 and GSU1501 (*xapC* and *xapD*) are highly conserved in six recently analyzed *Geobacter* genomes, with reciprocal orthologs in each (11). A similar genetic linkage also exists in *M. xanthus*, which has a cluster of ATP-dependent transporter genes (sharing as high as 40% identity with *xapBDE*) necessary for cell-cell cohesion and multicellular development immediately downstream of *M. xanthus* type IV pili (74).

The production of extracellular fibrils composed of protein and carbohydrate extending from *M. xanthus* is tightly regulated by pilus interactions via a complex signaling network known as the *dif* chemosensory pathway. An isolated matrix from *M. xanthus* causes pili to retract upon binding, and pilus retraction signals the *dif* pathway to increase matrix biosynthesis (6, 7, 39, 75). Comparative genomics of *Geobacter* has revealed a cluster of methyl-accepting chemotaxis proteins in the same gene order which are homologous to the *dif* proteins of *Myxococcus* (68). Future studies should focus on whether components of the *Geobacter xap* matrix signal type IV pili to retract, as this would have the benefit of bringing cells closer together for between-cell electron transfer. Also, if pili have an influence on *xap* matrix biosynthesis in *Geobacter*, then pilus mutants would be hypothesized to also be altered in this essential extracellular matrix that mediates cell surface attachment and cytochrome anchoring.

ACKNOWLEDGMENTS

J. B. Rollefson was supported by the Training for Biotechnology Development grant GM008347 from the National Institutes of Health. C. S. Stephen was supported by the Center for Environmental Kinetics Analysis (CEKA), funded by the National Science Foundation under grant no. CHE-0431328 and the Alfred P. Sloan Foundation Graduate Scholarship Program.

Guidance in SEM imaging was kindly provided by Aaron Barnes. We thank Meagan Aliff for help with preliminary SEM studies and Martin Dworkin for insightful comments.

REFERENCES

1. **Appenzeller, B. M. R., Y. B. Duval, F. Thomas, and J. Block.** 2002. Influence of phosphate on bacterial adhesion onto iron oxyhydroxide in drinking water. Environ. Sci. Technol. **36:**646–652.
2. **Araujo, J. C., et al.** 2003. Comparison of hexamethyldisilazane and critical point drying treatments for SEM analysis of anaerobic biofilms and granular sludge. J. Electron. Microsc. **52:**429–433.
3. **Arnold, J. W., and L. J. Shimkets.** 1988. Cell surface properties correlated with cohesion in *Myxococcus xanthus*. J. Bacteriol. **170:**5771–5777.
4. **Arnold, J. W., and L. J. Shimkets.** 1988. Inhibition of cell-cell interactions in *Myxococcus xanthus* by Congo red. J. Bacteriol. **170:**5765–5770.
5. **Behmlander, R. M., and M. Dworkin.** 1994. Biochemical and structural analyses of the extracellular matrix fibrils of *Myxococcus xanthus*. J. Bacteriol. **176:**6295–6303.
6. **Black, W. P., Q. Xu, and Z. Yang.** 2006. Type IV pili function upstream of the Dif chemotaxis pathway in *Myxococcus xanthus* EPS regulation. Mol. Microbiol. **61:**447–456.
7. **Black, W. P., and Z. Yang.** 2004. *Myxococcus xanthus* chemotaxis homologs DifD and DifG negatively regulate fibril polysaccharide production. J. Bacteriol. **186:**1001–1008.
8. **Bond, D. R., and D. R. Lovley.** 2003. Electricity production by *Geobacter sulfurreducens* attached to electrodes. Appl. Environ. Microbiol. **69:**1548–1555.
9. **Bradford, M. M.** 1976. A rapid and sensitive method for the quantification of microgram quantities of protein utilizing the principle of protein-dye binding. Anal. Biochem. **72:**248–254.
10. **Butler, J. E., F. Kaufmann, M. V. Coppi, C. Núñez, and D. R. Lovley.** 2004. MacA, a diheme *c*-type cytochrome involved in Fe(III) reduction by *Geobacter sulfurreducens*. J. Bacteriol. **186:**4042–4045.
11. **Butler, J. E., N. D. Young, and D. R. Lovley.** 2010. Evolution of electron transfer out of the cell: comparative genomics of six *Geobacter* genomes. BMC Genomics **11:**40.
12. **Caccavo, F. J., et al.** 1994. *Geobacter sulfurreducens* sp. nov., a hydrogen- and acetate-oxidizing dissimilatory metal-reducing microorganism. Appl. Environ. Microbiol. **60:**3752–3759.
13. **Chang, B., and M. Dworkin.** 1994. Isolated fibrils rescue cohesion and development in the Dsp mutant of *Myxococcus xanthus*. J. Bacteriol. **176:**7190–7196.
14. **Chen, X., and P. S. Stewart.** 2002. Role of electrostatic interactions in cohesion of bacterial biofilms. Appl. Microbiol. Biotechnol. **59:**718–720.
15. **Coppi, M. V., C. Leang, S. J. Sandler, and D. R. Lovley.** 2001. Development of a genetic system for *Geobacter sulfurreducens*. Appl. Environ. Microbiol. **67:**3180–3187.
16. **Cuthbertson, L., V. Kos, and C. Whitfield.** 2010. ABC transporters involved in export of cell surface glycoconjugates. Microbiol. Mol. Bio. Rev. **74:**341–362.
17. **Dan, N.** 2003. The effect of charge regulation on cell adhesion to substrates: salt-induced repulsion. Colloids Surf. B **27:**41–47.
18. **Danese, P. N., L. A. Pratt, and R. Kolter.** 2000. Exopolysaccharide production is required for development of *Escherichia coli* K-12 biofilm architecture. J. Bacteriol. **182:**3593–3596.
19. **Erlandsen, S. L., C. J. Kristich, G. M. Dunny, and C. L. Wells.** 2004. High-resolution visualization of the microbial glycocalyx with low-voltage scanning electron microscopy: dependence on cationic dyes. J. Histochem. Cytochem. **52:**1427–1435.
20. **Flemming, H., and J. Wingender.** 2010. The biofilm matrix. Nat. Rev. Microbiol. **8:**623–633.
21. **Fricke, K., F. Harnisch, and U. Schröder.** 2008. On the use of cyclic voltammetry for the study of anodic electron transfer in microbial fuel cells. Energy Environ. Sci. **1:**144–147.
22. **Holmes, D. E., et al.** 2006. Microarray and genetic analysis of electron transfer to electrodes in *Geobacter sulfurreducens*. Environ. Microbiol. **8:**1805–1815.
23. **Holmes, D. E., K. T. Finneran, R. A. O'Neil, and D. R. Lovley.** 2002. Enrichment of members of the family *Geobacteraceae* associated with stimulation of dissimilatory metal reduction in uranium-contaminated aquifer sediments. Appl. Environ. Microbiol. **68:**2300–2306.
24. **Huang, T., E. B. Somers, and A. C. L. Wong.** 2006. Differential biofilm formation and motility associated with lipopolysaccharide/exopolysaccharide-coupled biosynthetic genes in *Stenotrophomonas maltophilia*. J. Bacteriol. **188:**3116–3120.
25. **Inoue, K., et al.** 2010. Specific localization of the *c*-type cytochrome OmcZ at the anode surface in current-producing biofilms of *Geobacter sulfurreducens.* Environ. Microbiol. Rep. doi:10.1111/j.1758-2229.2010.00210.x.
26. **Inoue, K., et al.** 2010. Purification and characterization of OmcZ, an outer-surface, octaheme *c*-type cytochrome essential for optimal current production by *Geobacter sulfurreducens*. Appl. Environ. Microbiol. **76:**3999–4007.
27. **Keiski, C., et al.** 2010. AlgK is a TPR-containing protein and the periplasmic component of a novel exopolysaccharide secretin. Structure **18:**265–273.
28. **Klimes, A., et al.** 2010. Production of pilus-like filaments in *Geobacter sulfurreducens* in the absence of the type IV pilin protein PilA. FEMS Microbiol. Lett. **310:**62–68.
29. **Korenevsky, A., and T. J. Beveridge.** 2007. The surface physicochemistry and adhesiveness of *Shewanella* are affected by their surface polysaccharides. Microbiology **153:**1872–1883.
30. **Kouzuma, A., X. Meng, N. Kimura, K. Hashimoto, and K. Watanabe.** 2010. Disruption of the putative cell surface polysaccharide biosynthesis gene SO3177 in *Shewanella oneidensis* MR-1 enhances adhesion to electrodes and current generation in microbial fuel cells. Appl. Environ. Microbiol. **76:**4151–4157.
31. **Kovach, M. E., et al.** 1995. Four new derivatives of the broad-host-range

cloning vector pBBR1MCS, carrying different antibiotic-resistance cassettes. Gene **166:**175–176.
32. **Krushkal, J., et al.** 2010. Genome-wide survey for PilR recognition sites of the metal-reducing prokaryote *Geobacter sulfurreducens*. Gene **469:**31–44.
33. **Kus, J. V., et al.** 2008. Modification of *Pseudomonas aeruginosa* Pa5196 type IV pilins at multiple sites with D-Araf by a novel GT-C family arabinosyltransferase, TfpW. J. Bacteriol. **190:**7464–7478.
34. **Laemmli, U. K.** 1970. Cleavage of structural proteins during the assembly of the head of the bacteriophage T4. Nature **227:**680–685.
35. **Lancero, H., et al.** 2004. Characterization of a *Myxococcus xanthus* mutant that is defective for adventurous motility and social motility. Microbiology **150:**4085–4093.
36. **Leang, C., et al.** 2005. Adaptation to disruption of the electron transfer pathway for Fe(III) reduction in *Geobacter sulfurreducens*. J. Bacteriol. **187:** 5918–5926.
37. **Leang, C., M. V. Coppi, and D. R. Lovley.** 2003. OmcB, a *c*-type polyheme cytochrome, involved in Fe(III) reduction in *Geobacter sulfurreducens*. J. Bacteriol. **185:**2096–2103.
38. **Leang, C., X. Qian, T. Mester, and D. R. Lovley.** 2010. Alignment of the *c*-type cytochrome OmcS along pili of *Geobacter sulfurreducens*. Appl. Environ. Microbiol. **76:**4080–4084.
39. **Li, Y., et al.** 2003. Extracellular polysaccharides mediate pilus retraction during social motility of *Myxococcus xanthus*. Proc. Natl. Acad. Sci. U. S. A. **100:**5443–5448.
40. **Lloyd, J. R., et al.** 2003. Biochemical and genetic characterization of PpcA, a periplasmic *c*-type cytochrome in *Geobacter sulfurreducens*. Biochem. J. **369:**153–161.
41. **Lovley, D. R., and E. J. P. Phillips.** 1986. Organic matter mineralization with reduction of ferric iron in anaerobic sediments. Appl. Environ. Microbiol. **51:**683–689.
42. **Lower, B. H., et al.** 2009. Antibody recognition force microscopy shows that outer membrane cytochromes OmcA and MtrC are expressed on the exterior surface of *Shewanella oneidensis* MR-1. Appl. Environ. Microbiol. **75:** 2931–2935.
43. **Lowry, O. H., N. J. Rosebrough, A. L. Farr, and R. J. Randall.** 1951. Protein measurement with the Folin phenol reagent. J. Biol. Chem. **193:**265–275.
44. **Marshall, K. C., and M. R. Stout.** 1971. Mechanisms of the initial events in the absorption of marine bacteria to surfaces. J. Gen. Microbiol. **68:**337–348.
45. **Marshall, M. J., et al.** 2006. *c*-type cytochrome-dependent formation of U(IV) nanoparticles by *Shewanella oneidensis*. PLoS Biol. **4:**e268. doi: 10.1371/journal.pbio.0040268.
46. **Marsili, E., J. B. Rollefson, D. B. Baron, R. M. Hozalski, and D. R. Bond.** 2008. Microbial biofilm voltammetry: direct electrochemical characterization of catalytic electrode-attached biofilms. Appl. Environ. Microbiol. **74:**7329–7337.
47. **Marsili, E., J. Sun, and D. R. Bond.** 2010. Voltammetry and growth physiology of *Geobacter sulfurreducens* biofilms as a function of growth stage and imposed electrode potential. Electronanalysis **22:**865–874.
48. **Masuko, T., et al.** 2005. Carbohydrate analysis by a phenol-sulfuric acid method in microplate format. Anal. Biochem. **339:**69–72.
49. **Mayer, C., et al.** 1999. The role of intermolecular interactions: studies on model systems for bacterial biofilms. Int. J. Biol. Macromol. **26:**3–16.
50. **Mehta, T., M. V. Coppi, S. E. Childers, and D. R. Lovley.** 2005. Outer membrane *c*-type cytochromes required for Fe(III) and Mn(IV) oxide reduction in *Geobacter sulfurreducens*. Appl. Environ. Microbiol. **71:**8634–8641.
51. **Nevin, K. P., et al.** 2009. Anode biofilm transcriptomics reveals outer surface components essential for high density current production in *Geobacter sulfurreducens* fuel cells. PLoS One **4:**e5628.
52. **Nevin, K. P., and D. R. Lovley.** 2000. Lack of production of electron-shuttling compounds or solubilization of Fe(III) during reduction of insoluble Fe(III) oxide by *Geobacter metallireducens*. Appl. Environ. Microbiol. **66:**2248–2251.
53. **O'Toole, G. A., et al.** 1999. Genetic approaches to study of biofilms. Methods Enzymol. **310:**91–109.
54. **Palmer, J., S. Flint, and J. Brooks.** 2007. Bacterial cell attachment, the beginning of a biofilm. J. Ind. Microbiol. Biotechnol. **34:**577–588.
55. **Qiu, Y., et al.** 2010. Structural and operational complexity of the *Geobacter sulfurreducens* genome. Genome Res. **20:**1304–1311.
56. **Raven, K. P., A. Jain, and R. H. Loeppert.** 1998. Arsenite and arsenate adsorption on ferrihydrite: kinetics, equilibrium, and adsorption envelopes. Environ. Sci. Technol. **32:**344–349.
57. **Reguera, G., et al.** 2005. Extracellular electron transfer via microbial nanowires. Nature **435:**1098–1101.
58. **Reguera, G., et al.** 2006. Biofilm and nanowire production leads to increased current in *Geobacter sulfurreducens* fuel cells. Appl. Environ. Microbiol. **72:**7345–7348.
59. **Reguera, G., R. B. Pollina, J. S. Nicoll, and D. R. Lovley.** 2007. Possible nonconductive role of *Geobacter sulfurreducens* pilus nanowires in biofilm formation. J. Bacteriol. **189:**2125–2127.
60. **Richter, H., et al.** 2009. Cyclic voltammetry of biofilms of wild type and mutant *Geobacter sulfurreducens* on fuel cell anodes indicates possible roles of OmcB, OmcZ, type IV pili, and protons in extracellular electron transfer. Energy Environ. Sci. **2:**506–516.
61. **Rollefson, J. B., C. E. Levar, and D. R. Bond.** 2009. Identification of genes involved in biofilm formation and respiration via mini-*Himar* transposon mutagenesis of *Geobacter sulfurreducens*. J. Bacteriol. **191:**4207–4217.
62. **Rooney-Varga, J. N., R. T. Anderson, J. L. Fraga, D. Ringelberg, and D. R. Lovley.** 1999. Microbial communities associated with anaerobic benzene degradation in a petroleum-contaminated aquifer. Appl. Environ. Microbiol. **65:**3056–3063.
63. **Rosenberg, L.** 1971. Chemical basis for the histological use of safranin O in the study of articular cartilage. J. Bone Joint Surg. Am. **53:**69–82.
64. **Saltikov, C. W., and D. K. Newman.** 2003. Genetic identification of a respiratory arsenate reductase. Proc. Natl. Acad. Sci. U. S. A. **100:**10983–10988.
65. **Shimkets, L. J., and H. Rafiee.** 1990. CsgA, and extracellular protein essential for *Myxococcus xanthus* development. J. Bacteriol. **172:**5299–5306.
66. **Snoeyenbos-West, O. L., K. E. Nelson, R. T. Anderson, and D. R. Lovley.** 2000. Enrichment of *Geobacter* species in response to stimulation of Fe(III) reduction in sandy aquifer sediments. Microb. Ecol. **39:**153–167.
67. **Thomas, P. E., D. Ryan, and W. Levin.** 1976. An improved staining procedure for the detection of the peroxidase activity of cytochrome *P*-450 on sodium dodecyl sulfate polyacrylamide gels. Anal. Biochem. **75:**168–176.
68. **Tran, H. T., J. Krushkal, F. M. Antommattei, D. R. Lovley, and R. M. Weis.** 2008. Comparative genomics of *Geobacter* chemotaxis genes reveals diverse signaling function. BMC Genomics **9:**471.
69. **Vinogradov, E., A. Korenevsky, D. R. Lovley, and T. J. Beveridge.** 2004. The structure of the core region of the lipopolysaccharide from *Geobacter sulfurreducens*. Carbohydr. Res. **339:**2901–2904.
70. **Voisin, S., et al.** 2007. Glycosylation of *Pseudomonas aeruginosa* strain Pa5196 type IV pilins with mycobacterium-like α-1,5-linked D-Ara*f* oligosaccharides. J. Bacteriol. **189:**151–159.
71. **Voordeckers, J. W., B. Kim, M. Izallalen, and D. R. Lovley.** 2010. Role of *Geobacter sulfurreducens* outer surface *c*-type cytochromes in reduction of soil humic acid and anthraquinone-2,6-disulfonate. Appl. Environ. Microbiol. **76:**2371–2375.
72. **Vu, B., M. Chen, R. J. Crawford, and E. P. Ivanova.** 2009. Bacterial extracellular polysaccharides involved in biofilm formation. Molecules **14:**2535–2554.
73. **Watnick, P. I., and R. Kolter.** 1999. Steps in the development of a *Vibrio cholerae* El Tor biofilm. Mol. Microbiol. **34:**586–595.
74. **Wu, S. S., J. Wu, Y. L. Cheng, and D. Kaiser.** 1998. The *pilH* gene encodes an ABC transporter homologue required for type IV pilus biogenesis and social gliding motility in *Myxococcus xanthus*. Mol. Microbiol. **29:**1249–1261.
75. **Yang, Z., R. Lux, W. Hu, C. Hu, and W. Shi.** 2010. PilA localization affects extracellular polysaccharide production and fruiting body formation in *Myxococcus xanthus*. Mol. Microbiol. **76:**1500–1513.